High Energy Hadronic Interactions and Cosmic Ray Physics

G. Mitsuka
Solar-Terrestrial Environment Laboratory, Nagoya University
Furo-cho, Chikusa-ku, Nagoya, 464-8601, Japan

Interpretation of observations of ultra-high-energy cosmic rays relies on the knowledge about forward particle productions in hadronic interaction. Especially the choice of the hadronic interaction generator (model) in the Monte Carlo simulations of air shower development significantly affects the simulated results, and accordingly accelerator data on the production of very forward emitted particles are indispensable for constraining the hadronic interaction models. In this paper, recent progress in understanding of high energy hadronic interactions is discussed from the viewpoint of the cosmic ray observations.

1 Introductions

Measurements of the energy spectrum, chemical composition and arrival direction of ultra-high-energy cosmic rays ($E \gtrsim 10^{18}$ eV) are indispensable for understanding their origin and the high energy phenomena occurred in the universe. Huge experiments for observing extensive air showers, $E \gtrsim 10^{14}$ eV, have been operated and also provided valuable data so far. However the interpretation of these experimental air shower data to the primary cosmic ray parameters largely relies on our relatively poor knowledge of hadronic interaction in the earth's atmosphere at the corresponding energy scale.

A biggest open problem is the long standing question of the origin and the acceleration mechanism of the galactic cosmic rays [1]. In the "standard" scenario, supernova remnants can be a source of the galactic cosmic rays and the acceleration limit is thought to be $Z \times 10^{15}$ eV where Z is the charge of the primary cosmic ray. This scenario predicts a Z dependence of the cutoff energy for galactic cosmic rays. Determination of the chemical composition above $E > 10^{15}$ eV is important for confirming the standard scenario. The Pierre Auger Observatory [2], Telescope Array [3] and HiRes [4] have carried out precise measurements of the shower particles on the ground, however their interpretation highly depends on the choice of hadronic interaction generator employed in the air shower Monte Carlo (MC) simulations. Figures 1 show the $X_{\max}$ and RMS($X_{\max}$) distribution as a function of reconstructed cosmic ray energy together with the predictions of MC simulations. It is found that, for example, predicted $X_{\max}$ varies $\sim 50\,\mathrm{g/cm^2}$ for proton primaries and $\sim 30\,\mathrm{g/cm^2}$ for iron primaries at 4×10^{19} eV and such variation propagates into an uncertainty of the determination of chemical composition.

Even in other problems, i.e. energy spectrum and arrival direction, cosmic ray studies based on a large number of experimental data could be misinterpreted due to the uncertainty of the hadronic interaction generators in air shower MC simulations. These uncertainties can only be reduced by precise theoretical understanding of hadronic interaction and high energy accelerator experiments in the forward direction.

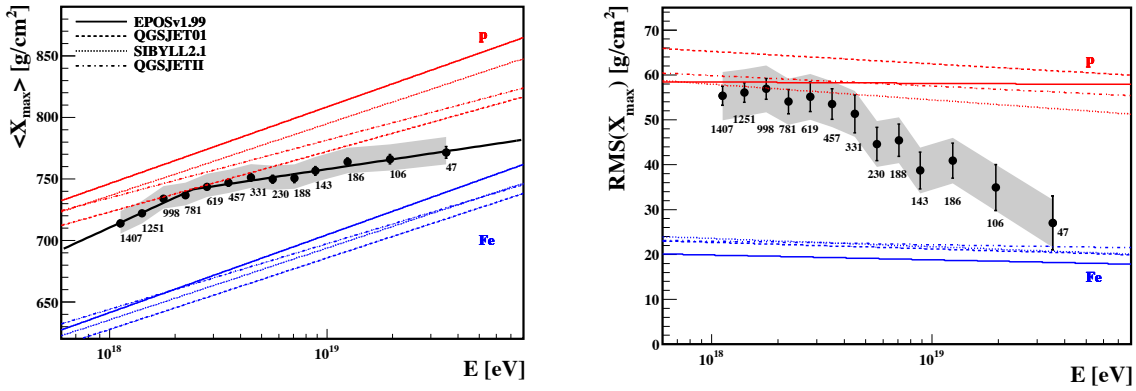

Figure 1: $X_{\rm max}$ (left) and RMS($X_{\rm max}$) (right) distribution obtained by the measurements by the fluorescence detector of the Pierre Auger Observatory. Measured data (closed circle) are shown with the predictions for proton and iron primary cosmic ray for several hadronic interaction generators. The number of events in each energy bin is also shown. Shaded area indicates the systematic uncertainties. Figures are taken from the Proceedings of ICRC 2011 [5].

This paper is organized as follows. Section 2 discusses how much high energy hadron production cross section can affect a determination of the origin of cosmic rays. In Section 3, an application of inclusive photon spectra 4 at the TeV energy scale to air shower simulation is discussed. Instead Section is assigned to the discussion of low-energy pion productions. Finally this paper is summarized in Section 5.

2 Hadron production cross section

Possible effects of an uncertainty of hadron production cross section on the determination of $X_{\rm max}$ and RMS($X_{\rm max}$) are investigated by R. Ulrich, R. Engel and M. Unger [6]. In this study, artificial modifications are applied to the secondary multiplicity, hadron production cross section, elasticity and pion charge-ratio in the SIBYLL model [13] and a large number of air showers are simulated by CONEX [8], where an artificial modification is formulated as

$$\begin{aligned} f(E, f_{19}) &= 1 + (f_{19} - 1)F(E), \\ F(E) &= \begin{cases} 0 & E \leqq 1\,\mathrm{PeV} \\ \frac{\log_{10}(E/1\,\mathrm{PeV})}{\log_{10}(10\,\mathrm{EeV}/1\,\mathrm{PeV})} & E > 1\,\mathrm{PeV}. \end{cases} \end{aligned} \tag{1}$$

The modification factor $f(E, f_{19})$ is getting larger as energy E above $E > 1\,\mathrm{PeV}$, while is set as 1 below $10^{15}\,\mathrm{eV}$ since this energy range has been studied by accelerator based experiments. f_{19} is the preassigned uncertainty at $10^{19}\,\mathrm{eV}$. Impact of modifications on $X_{\rm max}$ and RMS($X_{\rm max}$) are found in Figures 2. Largest systematic shift both on $X_{\rm max}$ and RMS($X_{\rm max}$) is caused by the uncertainty of hadron production cross section indicated by closed circle. For example factor ~ 3 increase of cross section at $E = 10^{19}\,\mathrm{eV}$ gives $-100\,\mathrm{g/cm^2}$ shift in the mean of $X_{\rm max}$ for proton primaries, thus they can be misidentified as iron primaries that have smaller $X_{\rm max}$ values. See the original document for detailed discussions about other many observables by air shower experiments.

3 Inclusive photon spectra

Figures 3 illustrate the impact of pion productions on air shower development. In left panel, X_F distributions of two different pion production models are presented within $0.01 < X_F < 1.0$:

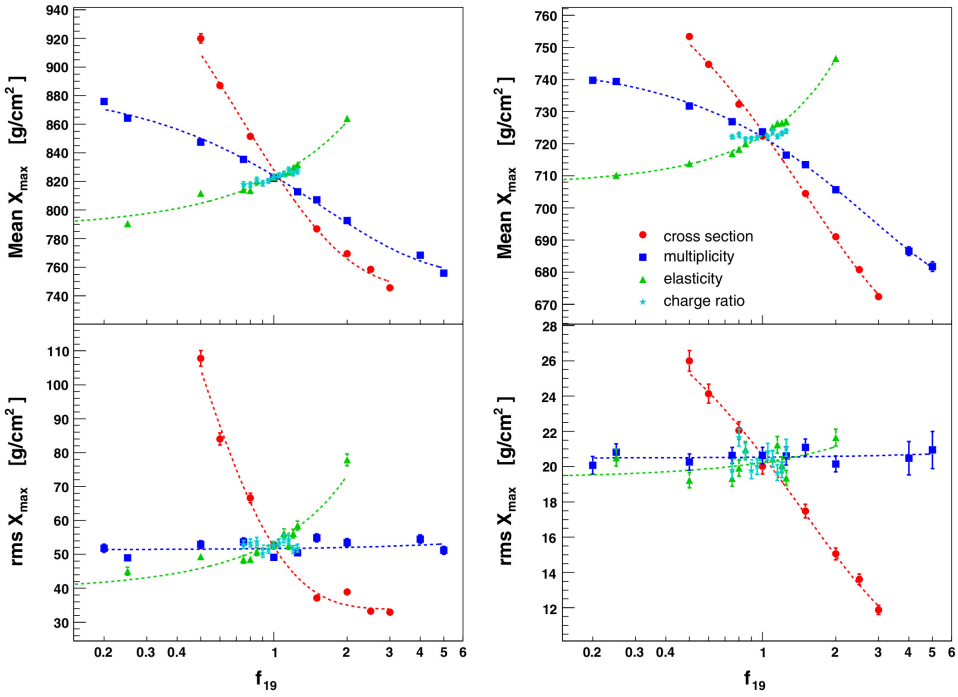

Figure 2: Impact of uncertainties in hadronic interactions on $X_{\max}$ and RMS($X_{\max}$). Left and right panel show the results with proton and iron primaries of the energy $10^{19.5}$ eV, respectively. Figures are taken from Phys. Rev. D **83**, 054026 (2011) [6].

ad-hoc model A (open circle) and ad-hoc model B (cross). Model A is supposed to carry out the primary energy into deeper in the atmosphere, while in model B energy is deposited earlier than model A. The number of electrons in air shower simulations with proton primaries with $E = 10^{17}$ eV are found in the right panel. There are two points to be noted. One is the effect to an absolute energy reconstruction; In case showers are detected at an altitude of 900 g/cm^2, energy can be misidentified by a factor of 1.75 between model A and B due to the difference of number of electrons at the detection level. Second is the effect to a determination of chemical composition using $X_{\max}$. $X_{\max}$ of model A is approximately 650 g/cm^2, while in model B $X_{\max}$ is $\sim$ 750 g/cm^2. The difference by $\sim$ 100 g/cm^2 is enough large to lead to a misconstruction of a kind of primary cosmic ray particle.

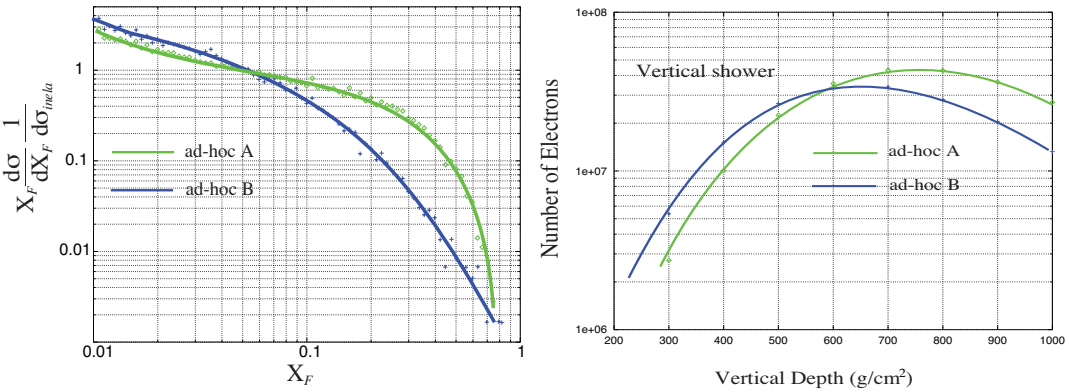

Figure 3: (Left) X_F distributions of two different pion production models. Open circle and cross indicate the ad-hoc model A and B, respectively. (Right) The number of electrons in air shower simulation based on ad-hoc model A (open circle) and B (cross). Figures are taken from the TDR of the LHCf experiment [9].

The Large Hadron Collider forward (LHCf) experiment [9] has been designed to measure the neutral particle (photon, π^0 and neutron) production cross sections at very forward collision angles of LHC proton-proton collisions. Study of inclusive photon spectra by LHCf [10] has been carried out in two pseudorapidity regions, $8.81 < \eta < 8.99$ and $\eta > 10.94$, in which photons are dominantly attributed to π^0 decay. Figures 4 show the LHCf measurements and the predictions of several hadronic interaction generators. Different colors show the results from LHCf data (black) and predictions by QGSJET II-03 [11] (blue), DPMJET 3.04 [12] (red), SIBYLL 2.1 [13] (green), EPOS 1.99 [14] (magenta) and PYTHIA 8.145 [15] (yellow). Error bars and gray shaded areas in each plot indicate the experimental statistical and the systematic errors, respectively. The magenta shaded area indicates the statistical error of the MC data set using EPOS 1.99 as a representative of the other models. Accordingly it is recognized that none of the generators lies within the errors of the LHCf photon spectra over the entire energy range.

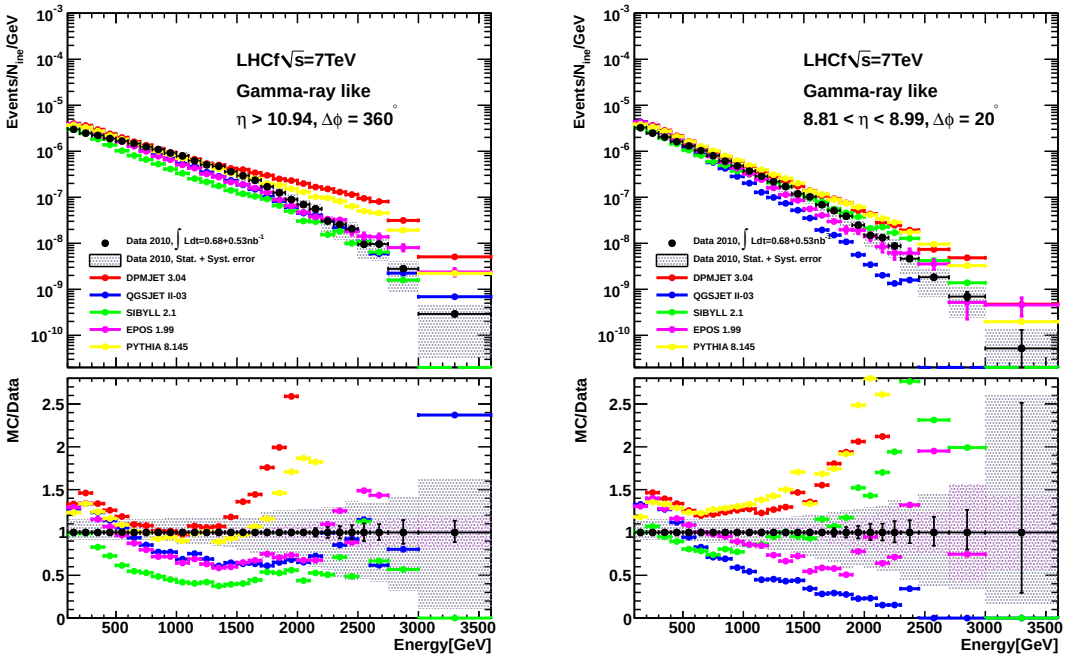

Figure 4: Comparison of the single photon energy spectra between the experimental data and the MC predictions. Top panels show the spectra and the bottom panels show the ratios of MC results to experimental data. Left (right) panel shows the results for the large (small) rapidity range. Figures are taken from Phys. Lett. B **703**, 128-134 (2011) [10].

4 Low energy hadronic interaction

The Pierre Auger Observatory has uses muons detected by their ground detectors for reconstructing the primary energy of cosmic ray. The mesons, dominantly pions, that decay into muons at the detection altitude are produced in the relatively low energy interactions ($E \sim 10 - 1000\,\mathrm{GeV}$) that correspond to the last interaction of air shower development. It is known that effects of low energy interactions to the entire uncertainty of the number of muons that can be detected at the ground level are larger than 10 % [16]. It is also reported that the excess of the number of muons at ground level compared to the prediction of air shower simulations causes the systematic uncertainty for the interpretation of the ultra-high-energy measurements. An proposed idea [17] is to enhance the production of (anti-)baryons in hadron-air interactions,

that is implemented in the EPOS hadronic interaction generator. Modeling of baryon productions in hadron-nucleus and nucleus-nucleus collisions can be tested using the measurements by the NA61/SHINE experiment [18].

The NA61/SHINE experiment aims an understanding of hadron productions in relatively low energy regions (proton beam $p < 158\,\mathrm{GeV}/c$). NA61 has taken data since 2007. Analysis of inclusive charged pion production is performed using the 2007 pilot run with $p + C$ interactions at $31\,\mathrm{GeV}/c$, and analysis results are compared with the predictions of low-energy hadronic interaction generators commonly used in air-shower MC simulations. Figures 5 show the charged pion spectra and predictions by FLUKA 2008 [19], URQMD 1.3.1 [20] and VENUS 4.12 [21] that are parts of the CORSIKA air shower simulation library [22]. It is recognized that the best agreement with the NA61 measurements is obtained by the FLUKA 2008 library.

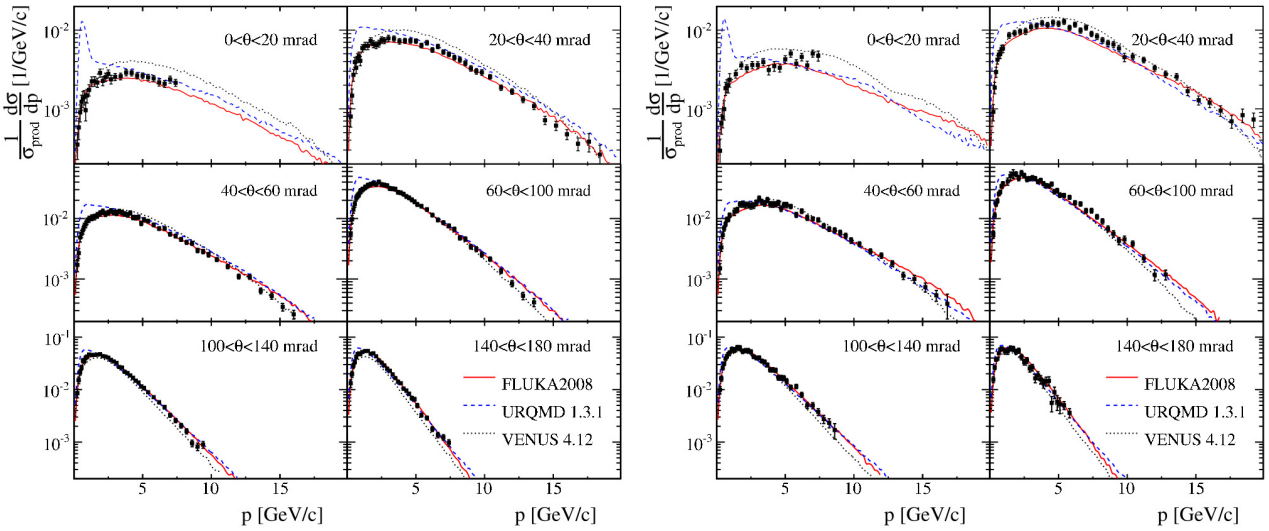

Figure 5: Charged pion productions in $p + C$ interactions at $31\,\mathrm{GeV}/c$, and simulated results by FLUKA 2008, URQMD 1.3.1 and VENUS 4.12. π^+ productions are shown in the left panel and π^- productions are shown in the right panel. Figures are taken from Phys. Rev. C **84**, 034604 (2011) [18].

5 Conclusions

The interpretation of observations of ultra-high-energy cosmic rays owe to knowledge of hadron productions in cosmic ray interaction in the atmosphere. As an example, there still exists a large systematic variation in $X_{\max}$ and RMS($X_{\max}$) especially in the energy range $E > 10^{18}\,\mathrm{eV}$, and this is responsible for somewhat poor understanding of chemical composition of ultra-high-energy cosmic rays. In this paper, possible reasons for systematic variations in the observables of air shower experiment are investigated within a few tens of GeV to EeV.

References

1. J. R. Hörandel, Astropart. Phys. **19**, 193–220 (2003).
2. J. Abraham, *et al.*, Phys. Rev. Lett., **104**, 091101 (2010).
3. H. Sagawa, AIPC, **1367**, 17-22, (2011).
4. R. U. Abbasi, *et al.*, Phys. Rev. Lett. **104**, 161101 (2010).
5. P. Facal Luis, Proceedings of the 32nd ICRC (2011).
6. R. Ulrich, R. Engel and M. Unger, Phys. Rev. D **83**, 054026 (2011).

7. E.-J. Ahn, R. Engel, T. K. Gaisser, P.Lipari and T. Stanev, Phys. Rev., **D80**, 094003 (2009).
8. T. Bergmann *et al.*, Astropart. Phys. **26**, 420-432 (2007). T. Pierog *et al.*, Nucl. Phys. Proc. Suppl. **151**, 159-162 (2006).
9. The LHCf Collaboration, CERN-LHCC-2006-004, LHCF-TDR-001, **7** (2006).
10. O. Adriani *et al.* (The LHCf Collaboration), Phys. Lett. B **703**, 128-134 (2011).
11. S. Ostapchenko, Phys. Rev., **D74**, 014026 (2006).
12. F. W. Bopp, J. Ranft R. Engel and S. Roesler, Phys. Rev., **C77**, 014904 (2008).
13. E.-J. Ahn, R. Engel, T. K. Gaisser, P.Lipari and T. Stanev, Phys. Rev., **D80**, 094003 (2009).
14. K. Werner, F.-M. Liu and T. Pierog, Phys. Rev., **C74**, 044902 (2006).
15. T. Sjöstand, S. Mrenna and P. Skands, JHEP05, 026 (2006). T. Sjöstand, S. Mrenna and P. Skands, Comput. Phys. Comm., **178**, 852 (2008).
16. M. Unger *et al.*, Proceedings of the 32nd ICRC (2011).
17. T. Pierog and K. Werner, Phys. Rev. Lett. **101**, 171101 (2008).
18. N. Abgrall *et al.* (The NA61/SHINE Collaboration), Phys. Rev. C **84**, 034604 (2011).
19. G. Battistoni, S. Muraro, P.R. Sala, F. Cerutti, A. Ferrari, S. Roesler, A. Fasso', J. Ranft, AIP Conference Proceeding 896, 31-49, (2007). A. Ferrari, P.R. Sala, A. Fasso', and J. Ranft, CERN-2005-10 (2005), INFN/TC_05/11, SLAC-R-773.
20. M. Bleicher *et al.*, J. Phys. G: Nucl. Part. Phys. **25**, 1859 (1999).
21. K. Werner, Nucl. Phys. A **525**, 501c (1991), K. Werner, Phys. Rep. **232**, 87 (1993).
22. D. Heck *et al.*, Report FZKA 6019 (1998).